© 2011 by The American Society for Biochemistry and Molecular Biology, Inc.
This paper is available on line at http://www.mcponline.org

Profiling Cys^{34} Adducts of Human Serum Albumin by Fixed-Step Selected Reaction Monitoring*[S]

He Li‡, Hasmik Grigoryan‡, William E. Funk§, Sixin Samantha Lu‡, Sherri Rose‡, Evan R. Williams¶‡, and Stephen M. Rappaport‡‖

A method is described for profiling putative adducts (or other unknown covalent modifications) at the Cys^{34} locus of human serum albumin (HSA), which represents the preferred reaction site for small electrophilic species in human serum. By comparing profiles of putative HSA-Cys^{34} adducts across populations of interest it is theoretically possible to explore environmental causes of degenerative diseases and cancer caused by both exogenous and endogenous chemicals. We report a novel application of selected-reaction-monitoring (SRM) mass spectrometry, termed fixed-step SRM (FS-SRM), that allows detection of essentially all HSA-Cys^{34} modifications over a specified range of mass increases (added masses). After tryptic digestion, HSA-Cys^{34} adducts are contained in the third largest peptide (T3), which contains 21 amino acids and an average mass of 2433.87 Da. The FS-SRM method does not require that exact masses of T3 adducts be known in advance but rather uses a theoretical list of T3-adduct *m/z* values separated by a fixed increment of 1.5. In terms of added masses, each triply charged parent ion represents a bin of ±2.3 Da between 9.1 Da and 351.1 Da. Synthetic T3 adducts were used to optimize FS-SRM and to establish screening rules based upon selected *b*- and *y*-series fragment ions. An isotopically labeled T3 adduct is added to protein digests to facilitate quantification of putative adducts. We used FS-SRM to generate putative adduct profiles from six archived specimens of HSA that had been pooled by gender, race, and smoking status. An average of 66 putative adduct hits (out of a possible 77) were detected in these samples. Putative adducts covered a wide range of concentrations, were most abundant in the mass range below 100 Da, and were more abundant in smokers than in nonsmokers. With minor modifications, the FS-SRM methodology can be applied to other nucleophilic sites and proteins. ***Molecular & Cellular Proteomics 10: 10.1074/mcp.M110.004606, 1–13, 2011.***

Reactive electrophiles, particularly aldehydes, epoxides, quinones, and short-lived oxygen and nitrogen species, have long been implicated as causes of major human diseases (1–5). These electrophiles enter the blood following metabolism of exogenous compounds, from oxidation of lipids and other natural molecules, from ionizing radiation, and from inflammation associated with infections and disease processes. Because of their short life spans *in vivo*, it is rarely possible to measure reactive electrophiles in body fluids. However, adducts produced by reactions with blood nucleophiles, notably hemoglobin (Hb)[1] and human serum albumin (HSA), reflect the presence of reactive electrophiles in the systemic circulation (6, 7). Levels of targeted Hb and/or HSA adducts have been investigated in human blood for several exogenous or endogenous toxicants that are either electrophilic carcinogens or their precursors, notably, acrylamide, aflatoxin B1, benzene, 1,3-butadiene, ethylene oxide, as well as assorted aromatic amines, polycyclic aromatic hydrocarbons, and aldehydes (from lipid peroxidation) [reviewed in (7)]. Some of these studies have shown strong correlations between levels of Hb and HSA adducts and the corresponding exposure levels of precursor molecules.

Recently, the concept of profiling essentially all covalent adducts bound to a given blood nucleophile, has been offered as an avenue for characterizing *unknown* reactive electrophiles in the systemic circulation (7–10). By comparing putative adduct profiles across populations of interest, such as in case/control studies, it is possible to pinpoint differences of potential health importance and thereby motivate additional experiments that seek accurate masses and structural information for identifying key electrophiles. Previous human applications of adduct profiling have focused upon either gluta-

From the ‡Center for Exposure Biology, University of California, Berkeley, CA 94720, USA, §Gillings School of Global Public Health, University of North Carolina, Chapel Hill, NC 27599, USA, ¶Department of Chemistry, University of California, Berkeley, CA 94720, USA

Received August 29, 2010, and in revised form, December 29, 2010
Published, MCP Papers in Press, December 30, 2010, DOI 10.1074/mcp.M110.004606

[1] The abbreviations used are: B, black; EstroT3, estrogen quinone-T3; Estro(re)T3, estrogen quinone (reduced form)-T3; F, female; FS-SRM, fixed-step selected reaction monitoring; FWHM, full width at half maximum; Hb, hemoglobin; HSA, human serum albumin; IAA, iodoacetamide; iT3, isotopically labeled T3; M, male; N, nonsmoker; NaphT3, 1,4-naphthquinone-T3; Q1, quadrupole 1; PhenT3, 1,2-phenanthrone-T3; Q3, quadrupole 3; S, smoker; SRM, selected reaction monitoring; TQ, triple quadrupole; W, white; HPLC, high performance liquid chromatography; ESI, electrospray ionization; BSA, bovine serum albumin; TCEP, tris(2-carboxyethyl)phosphine.

thione adducts (present as mercapturic acids) in urine (11, 12) or DNA adducts in postmortem tissues (8, 13). In both cases, putative adducts were profiled via high performance liquid chromatography (HPLC)-triple quadrupole (TQ)-mass spectrometry (MS) in selected reaction monitoring (SRM) mode. By scanning sequential lists of *theoretical* transitions, these investigators characterized essentially all detectable glutathione or DNA modifications within a specified range of mass increases (added masses). We refer to this novel TQ-MS approach for characterizing unknown analytes as "fixed-step SRM" (FS-SRM).

Although highly original, these previous FS-SRM applications have practical limitations for profiling putative adducts. First, because the ultimate goal is to compare profiles across human populations, intraindividual variability in adduct levels increases background noise, thereby obscuring differences. Thus, glutathione adducts, whose levels change dramatically even during a single day (12), are too transient for profiling studies, except possibly to evaluate short-term effects of diet or drugs or in situations where an adduct is generated continuously. Second, the nucleophilic target should permit putative adducts to be profiled in small volumes of blood. Because about 20 ml of blood is required to provide sufficient DNA for a single assay (100 μg) from nucleated blood cells, DNA is not a practical sample matrix for adduct profiling. This is probably why Kanaly *et al.* used autopsy specimens rather than blood as sources for DNA (8, 13). A more logical choice of a blood nucleophile would be either Hb (mean residence time = 60 d, 150 mg/ml blood) or HSA (mean residence time = 28 d, 30 mg/ml blood) (6, 7). Indeed, a drop or two of blood (50–100 μl) should suffice for adduct profiling with Hb or HSA.

Because of their strong nucleophilicity, free thiols in Cys residues of proteins are attractive targets for reactions with electrophiles. Interestingly, human Hb and HSA each have only one free thiol available for reaction, *i.e.* Hb-Cys$^{93\beta}$ and HSA-Cys^{34}. Because we had previously observed that specific xenobiotic adducts of HSA-Cys^{34} were present at much higher concentrations than those of Hb-Cys$^{93\beta}$ in human blood (14–16), we chose HSA-Cys^{34} for profiling experiments. In fact, HSA-Cys^{34} is a well known scavenger of small electrophiles that accounts for about 80% of all free thiols in human serum (17, 18), and HSA-Cys^{34} adducts have been unambiguously detected from reactions with aldehydes, nitrogen mustards, oxiranes, quinones, metal ions, and a host of drugs [reviewed in (7)]. Following tryptic digestion of HSA, all thiol adducts should be bound to a single peptide, which we designate as T3 (the third largest tryptic peptide of HSA), with sequence ALVLIAFAQYLQQC^{34}PFEDHVK and an average mass of 2433.87 Da.

Our focus upon adducts of a relatively large peptide (T3) introduces complexity into FS-SRM experiments. Previous applications involved small molecules, detected as adducted mercapturic acids (11, 12) or DNA nucleosides (8, 13), either of which permitted constant neutral losses to be used for theoretical transitions. By contrast, fragmentation of adducted peptides generally occurs at amide bonds that produce series of *b* and *y* fragment ions without prominent and reliable constant neutral losses. In order to confirm the presence of a given peptide adduct it is desirable to detect three or four characteristic *b* or *y* fragment ions (sequence tags) (19). With *a priori* lists containing hundreds of theoretical adducted peptides, this need for confirmatory sequence tags multiplies the transition list severalfold, thereby increasing the demands for spectral processing and data analysis.

Here, we describe a FS-SRM method to profile putative T3 adducts of HSA-Cys^{34} in chromatographic fractions of tryptic HSA digests. (Hereafter, we use the term "adduct" to refer to a chemical modification of HSA-Cys^{34} and not necessarily to imply an addition product at that locus). Using synthetic standards of T3 adducts, we demonstrate that FS-SRM can detect these species with high sensitivity and specificity, and we investigate potential false positives caused by abundant T3 adducts that "overflow" into adjacent added-mass bins. Finally, we apply the FS-SRM method to archived HSA samples that had previously been enriched for Cys^{34} adducts by treatment with a thiol affinity resin to remove mercaptalbumin (20). This permitted us to visualize the added-mass range and abundance of putative adducts in archived specimens of HSA from subjects stratified by race, gender, and smoking status.

EXPERIMENTAL PROCEDURES

Chemicals and Reagents—Acetic acid, acetone, acetonitrile, ammonium sulfate, calcium chloride, formic acid, hydrogen peroxide, iodoacetamide (IAA), methanol, methyltrioxorhenium, nitrosodisulfonate, sodium chloride, tris, and tris(2-carboxyethyl)phosphine were from Fisher Scientific (Pittsburgh, PA). 1,4-Benzoquinone, 1,4-naphthoquinone, estradiol, bovine serum albumin (BSA) and porcine trypsin were from Sigma-Aldrich (St. Louis, MO). 1,2-Phenanthrone was custom synthesized at the Midwest Research Institute (MRI, Camp LeJeune, NC). Water was purified to a resistivity of 18.2 MΩ cm (at 25 °C) using a Milli-Q Gradient ultrapure water purification system (Millipore, Billerica, MA). Synthetic T3 peptide was custom synthesized by Biomatik (Wilmington, DE). Isotopically labeled T3 (iT3) with sequence AL-[^{15}N,^{13}C-Val]-LIAFAQYLQQCPFEDH-[^{15}N,^{13}C-Val]-K was custom synthesized by BioMer Technology (Pleasanton, NY).

Analytical Scheme—Fig. 1 shows our scheme for enriching, purifying, and profiling putative HSA-Cys^{34} adducts. Because unadducted HSA-Cys^{34} (mercaptalbumin) readily binds to thiol trapping reagents, we use a thiol-affinity resin to remove mercaptalbumin and thereby to enrich HSA-Cys^{34} adducts prior to analysis (20). After digesting the adduct-enriched HSA with trypsin, we add an isotopically labeled T3 adduct of IAA as internal standard (IAA-iT3) for quantification of putative adducts. Modified T3 peptides are then purified by off-line HPLC and analyzed by TQ-MS using FS-SRM. Results of FS-SRM are displayed in profiles of putative adduct concentration *versus* added mass.

Synthesis of Estrogen Quinones—An isomeric mixture of 2,3-estrogen quinone and 3,4-estrogen quinone was prepared by dissolving 7 mg of estradiol in 2.8 ml acetone and diluting with 4.2 ml of 10% acetic acid. Following addition of 50 mg of nitrosodisulfonate, the mixture was incubated for 15 min at room temperature with continuous agitation. An additional 50 mg of nitrosodisulfonate were added

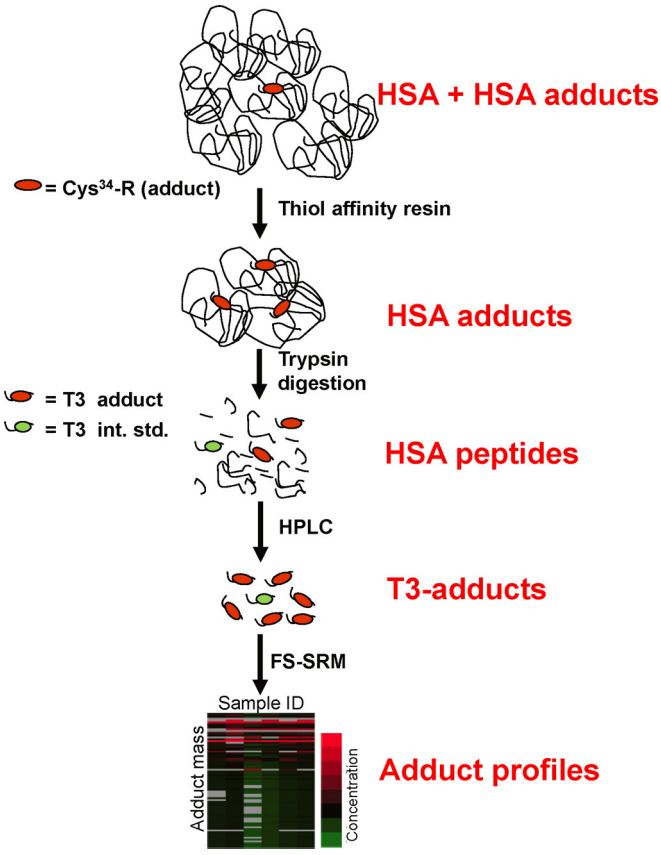

FIG. 1. **Scheme for enriching, purifying and profiling HSA-Cys^{34} adducts.** Thiol-affinity resins are used to remove mercaptalbumin (*i.e.* HSA containing free Cys^{34}). Enriched HSA-Cys^{34} adducts (and other covalent modifications) are purified by HPLC, detected as modified T3 peptides by FS-SRM, and displayed as a profile of T3-adduct concentration *versus* adduct mass.

to the reaction mixture with continuous agitation for another 15 min. The resulting isomeric mixture, containing 2,3-estrogen quinone and 3,4-estrogen quinone at a combined yield of greater than 95% [as determined by TQ-MS operating in selected-ion-monitoring mode], was extracted two times with 5 ml chloroform and the extract was dried under a gentle stream of nitrogen. The product was dissolved in 100 μl of methanol.

Synthesis and Purification of T3 Adducts—A stock solution of T3 was prepared by dissolving synthetic T3 in dimethylsulfoxide at 5 mM, followed by dilution with either water or methanol to a final concentration of 100 μM. A carboxyamidomethylated Cys^{34} adduct of T3 (IAA-T3) was prepared by adding IAA to 0.5 ml of 100 μM T3 stock solution to a final IAA concentration of 100 mM. The reaction mixture was incubated at 25 °C in the dark for 6 h with continuous agitation. The yield of IAA-T3 was determined using SRM to detect ions corresponding to T3 (average *m/z* 812.3, +3) and IAA-T3 (average *m/z* 831.3, +3). The isotopically labeled T3 (iT3) was modified with IAA in the same way to produce the internal standard, IAA-iT3. Following HPLC purification, a stock solution of IAA-iT3 was obtained at 32 μM in 35% acetonitrile, 0.1% formic acid.

The sulfonic acid of T3 (addition of 3 oxygen atoms) was synthesized by incubating 200 μl of 100 μM T3 stock solution in methanol with 2 μl of 100 mM H_2O_2 and 1 mM methyltrioxorhenium at room temperature with continuous agitation for 1 h. Adducts of T3 with 1,4-benzoquinone, 1,4-naphthoquinone, 1,2-phenanthrone, and the isomeric mixture of estrogen quinones were prepared by incubating each quinone or mixture at fivefold molar excess with 100 μM T3 in methanol at room temperature for 6 h with continuous agitation.

All synthetic T3 adducts were purified by reverse phase-HPLC with a UV detector at 280 nm (Agilent Technologies, Santa Clara, CA). Approximately 25 μg of each T3 adduct in 500 μl of 0.1% aqueous formic acid was injected via a manual injector (7725i, Rheodyne, equipped with a 1-ml stainless steel sample loop) onto a C18 column (5 μm, 250 mm × 4.6 mm, 300Å, Grace, Deerfield, IL) at a flow rate of 0.5 ml/min with a 15-min linear gradient of 5–90% acetonitrile/0.1% formic acid. The volume of the fraction containing each T3 adduct was 0.5–0.55 ml. The yield of each T3 adduct was determined by TQ-MS-SRM to be between 75 and 95%. Examining the end products of estrogen quinone-T3 adduction by high-resolution mass spectrometry revealed a mixture of T3 adducts consisting of estrogen quinone-T3, the diol of estrogen quinone-T3, and a minor (~2% of estrogen quinone) T3 adduct with a mass corresponding to the estrogen quinone plus 16 Da. Although the chemical structure of this minor adduct is not known, it is reasonable to assume that an oxygen atom was introduced into the estrogen quinone during synthesis. Adducted T3 peptides were stored in glass vials at −80 °C prior to use.

Mass Spectrometry—Collision induced dissociation experiments with synthetic T3 and its adducts and all SRM experiments were performed with a TQ-MS (Quantum Ultra TQ MS, Thermo Fisher Scientific, Waltham, MA), connected to an automated, chip based, nano-electrospray ionization (ESI) device (Tiversa Nanomate, Advion BioSciences, Ithaca, NY). Each sample was statically infused into the MS source via a conductive tip connected to a disposable nano-ESI-chip with an array of 20 × 20 silicon nozzles (5-μM i.d.). A voltage of 1.5 kV was applied to the nano-ESI tip, which was supplied with nitrogen at 0.4 bar. Each sample used a separate nano-ESI tip and spray nozzle to eliminate cross contamination. The mass spectrometer was tuned in SRM mode using T3. SRM data were acquired with both Q1 and Q3 resolution of 0.7 full width at half maximum (FWHM) a scan width of 0.002 *m/z*, and a dwell time of 0.02 s for each transition. Static infusion continued for sufficient time to obtain 200 repeat scans of each transition on the FS-SRM list (this number of repeat scans was found to be optimal based upon statistical criteria in preliminary experiments). Collision energies were optimized based on analysis of a set of synthetic T3 adducts (described in Results).

Fixed-Step SRM of T3 Adducts—Parent ions used in all FS-SRM experiments were in the *m/z* range between 815.0 and 929.0 with a fixed-step increment of 1.5 *m/z*. The transition list was generated by assuming that all theoretical parent ions were triply charged, in which case the adduct mass would be [(parent ion *m/z*)×3–3.03]-[2433.87–1.01], where 2433.87 Da is the average mass of T3 and 1.01 Da is the average mass of the hydrogen lost from the sulfhydryl group. Added masses were used to calculate the y_{15}^{2+}, y_{16}^{2+}, and y_{17}^{2+} product ion *m/z* values for the corresponding parent ions. The resulting FS-SRM transition list included 77 theoretical parent ions, each with four product ions, namely b_4^+ (universal to all T3 related peptides) and y_{15}^{2+}, y_{16}^{2+}, and y_{17}^{2+}(unique to each parent ion). Each triply charged parent ion represented an added-mass bin of ±2.3 Da (±0.75 *m/z*) between 9.1 Da and 351.1 Da. Because the y_{15}^{2+}, y_{16}^{2+}, and y_{17}^{2+}fragments contain modifications to Cys^{34}, their theoretical *m/z* values were determined by the theoretical added masses, whereas the theoretical b_4^+ fragment was common to all T3 parent ions. After including transitions for IAA-iT3 (internal standard), the queried list included a total of 312 transitions. Although this FS-SRM transition list permits detection of all modified T3 peptides with added masses between 9.1 Da and 351.1 Da, it provides no adduct-specific mass information, and adducts with similar masses could share the same bin.

Given a dwell time of 0.02 s and 200 measurements for each of 312 transitions, a FS-SRM required 21 min for data acquisition. The full FS-SRM transition list is given in Supplemental Information, supplemental Table S1. Adduct concentrations were calculated based on the signal intensity ratio of the most abundant fragment (y_{16}^{2+}) to that of the IAA-iT3 (internal standard); that is adduct concentration = (y_{16}^{2+} abundance of analyte/y_{16}^{2+} abundance of IAA-iT3) × concentration of IAA-iT3. To determine FS-SRM measurement variability, a sample consisting of 50 nM each of 1,4-benzoquinone-T3 and IAA-iT3 was measured 6 times. The coefficient of variation of the ratio of y_{16}^{2+} abundance of the ion representing1,4-benzoquinone-T3 to the corresponding y_{16}^{2+} abundance of IAA-iT3 was 2.1%.

Experiments with experimental samples showed prominent T3 adducts in bins with added masses of 22.6 Da, representing sodiated T3 (theoretical average added mass: 23.0 Da) and 58.6 Da, representing carboxyamidomethylated T3 (theoretical average added mass: 58.1 Da), which was produced by reaction of T3 with residual IAA in the internal standard solution. Thus, T3 adducts with added masses of 22.6 Da and 58.6 Da were excluded from consideration. For investigating the effect of adduct concentration on FS-SRM "bin overflow" (discussed later), a stock solution of 1,4-benzoquinone-T3 in methanol was diluted with 50% acetonitrile, 0.1% formic acid to desired concentrations between 0.5 and 500 nM (in triplicate). The accuracy of FS-SRM for detecting targeted adducts was investigated with a mixture (in duplicate) of synthetic adducts consisting of the sulfonic acid of T3 (50 nM), 1,4-benzoquinone-T3 (70 nM), 1,2-phenanthrone-T3 (85 nM), and an isomeric mixture of 2,3- and 3,4-estrogen quinone-T3 (12.5 nM) and the diol of estrogen quinone-T3 (50 nM), plus IAA-iT3 (internal standard, 50 nM) in 50% acetonitrile, 0.1% formic acid.

Fixed-Step SRM of HSA-Cys^{34} Adducts from Human Blood—For profiling HSA-Cys^{34} adducts, FS-SRM data were acquired from archived samples of HSA that had been isolated, enriched for HSA-Cys^{34} adducts, and purified by HPLC as described below.

1) Isolation of HSA from Blood—Blood was obtained with informed consent from healthy subjects according to human-subject protocols approved by the University of North Carolina. After removing blood cells, ammonium sulfate was added to a final concentration of 60% to precipitate immunoglobulins and the remaining proteins were exhaustively dialyzed against water, lyophilized, and dissolved in water at 50 mg/ml (14). The current investigation of these archived proteins was conducted following 13 y of storage at −80 °C. Selected specimens were stratified and pooled with 5 subjects per pool based on gender, smoking status and race (white or black). The mean purity of HSA in these samples was determined for the current study as 46.9% by gel electrophoresis (20). The pooled HSA samples were maintained at −80 °C until further processing.

2) Enrichment of HSA-Cys^{34} Adducts—Eight pooled HSA samples were enriched for HSA-Cys^{34} adducts, including duplicates for male white smokers (MWS) and nonsmokers (MWN), and one sample each for female black smokers (FBS) and nonsmokers (FBN), and male black smokers (MBS) and nonsmokers (MBN). Each sample, containing 4 mg of pooled protein (of which ~2 mg was HSA) was incubated overnight with 300 mg (dry mass) of activated Thio Sepharose 4B (GE Healthcare, Buckinghamshire, UK) in degassed binding buffer (100 mM Tris-HCl, 0.5 M NaCl, pH 7.4). The resin was prepared in a ratio of 75% settled medium to 25% buffer in a 1.5-ml polypropylene spin tube with a 0.22-μm pore size (Pierce Spin Cups, Thermo Scientific, Pittsburgh, PA). Following incubation with the resin, the mixture was centrifuged and the flow-through fraction, containing HSA-Cys^{34} adducts, was buffer-exchanged to 50 mM Tris-Cl (pH 8.0) using a centrifugal filter with a molecular weight cutoff of 10,000 Da (Sartorius, Goettingen, Germany). The adduct-enriched protein samples contained ~1.5 mg of protein, as determined by the Bradford assay (Bio-Rad, Hercules, CA) and approximately1.0 mg HSA, as determined by gel electrophoresis (20). Samples were stored at −80 °C until enzymatic digestion.

3) Enzymatic Digestion of Adduct-Enriched Protein—Pressure-assisted enzymatic digestion was performed to generate tryptic peptides of the adduct-enriched protein. Samples containing 0.5 mg of adduct-enriched protein (including ~0.34 mg of adducted HSA) were diluted with Tris-Cl buffer (pH 8.0) to ~440 μl. Then sufficient methanol and 200 mM tris(2-carboxyethyl)phosphine (TCEP) were added to give final concentrations of 10% methanol and 2 mM TCEP. The mixture was incubated at 37 °C for 15 min with gentle shaking. Following adding sufficient 200 mM aqueous $CaCl_2$ to give a final concentration of 2 mM $CaCl_2$, trypsin was added at a 1:30 ratio (trypsin:protein, w/w). The final volume of the digestion mixture was 500 μl. The digestion was carried out at 55 °C in a pressurized system (Barocycler NEP2320, Pressure Biosciences Inc., South Easton, MA), with pressure cycled between ambient and 1380 bar at 1 min intervals for 10 min. Following digestion, samples were transferred to 600-μl centrifuge tubes (Fisher, Pittsburg, PA) and 120 pmol IAA-iT3 (internal standard) was added.

4) HPLC Purification of T3 Adducts from Tryptic Digests—Immediately following digestion, T3 adducts were purified by HPLC (1100 Series, Agilent Technologies, Santa Clara, CA) using a UV detector at 280 nm, a *manual injector* (7725i, Rheodyne, equipped with a 1-ml stainless steel sample loop), a C8 reverse phase column (Vydac 208MS, C8, 5 μm, 250 mm × 4.6 mm, Grace) and a C8 guard column (Vydac 208MS, C8, 5 μm, 7.5 × 4.6 mm, Grace). Solvent A was 0.1% aqueous formic acid and solvent B was 99.9% acetonitrile with 0.1% formic acid (v/v). The entire 500 μl of the tryptic digest, containing ~0.5 mg of the tryptic peptides (representing ~0.34 mg of adducted HSA) and 120 pmol of IAA-iT3 (internal standard), were injected into the system at a flow rate of 500 μl/min. The elution gradient was as follows: 5% B initial condition; linear gradient from 5% B to 27% B in 5 min; hold at 27% B for 5 min; linear gradient from 27% to 70% B in 5 min; and hold at 70% B for 10 min. The optimal conditions for eluting the T3 adduct fraction were determined by injecting synthetic T3 peptides (T3, IAA-T3, 1,2-phenanthrone-T3, and estrogen-quinone T3). The HPLC fraction containing T3 adducts was collected from 19.6 to 22 min (1.2 ml). The final concentration of the internal standard in the collected fractions was 100 nM. Eluates were stored at −80 °C prior to mass spectrometry. Purified tryptic peptides from human samples were submitted for FS-SRM in random order.

Bovine Serum Albumin (BSA) as a Negative Control—We selected BSA as a negative control for FS-SRM experiments because it is homologous to HSA (including a free Cys^{34}) and would, therefore, behave similarly to HSA in all steps involving adduct enrichment, digestion, HPLC purification and TQ-MS. Yet, the T3-homologous peptide of BSA has the amino acid sequence of GLVLIAFSQYLQQC^{34}FFDEHVK (compared with ALVLIAFAQYLQQC^{34}PFEDHVK for HSA) and none of the four fragment ions used as sequence tags for HSA-T3 (b_4^+, y_{15}^{2+}, y_{16}^{2+}, and y_{17}^{2+}) has the same amino acid sequence as HSA-T3. A 2-mg portion of commercial BSA was carried through all procedures to enrich, digest, and purify Cys^{34} T3 adducts and then to monitor all theoretical transitions in FS-SRM experiments.

Data Analysis—Raw data files collected in SRM experiments were converted to mzXML data format using Trans Proteomic Pipeline v4.3 and were processed using ReadmzXML (open source software from the Institute for Systems Biology, Seattle, WA) to convert all transitions and their corresponding scan sequences and signal intensities to TXT files. An in-house MATLAB (The MathWorks, Natick, MA) program was written to apply screening rules (described in Results) to determine whether a given parent ion in a SRM experiment should be designated as a putative Cys^{34} T3 adduct and to perform statistical calculations. All data analyses used estimated geometric mean values

and their 95% confidence intervals from the 200 scan repeats for each transition in concurrent experimental and control (BSA) samples. For duplicate samples, only parent ions that were detected in both samples were accepted. Spearman correlation coefficients and coefficients of variation were estimated with SAS software (SAS for Windows, v. 9.2, Cary, NC). Adduct maps were generated using Cluster 3.0 and Java TreeView (21, 22).

RESULTS

Selection of SRM Transitions to Detect T3 Adducts—ESI of the T3 peptides resulted in predominantly triply protonated molecules. Fragment ions used in SRM experiments to detect T3 modifications were selected based on MS/MS spectra of unadducted T3 and a series of T3 adducts acquired by TQ-MS. As shown in Fig. 2, unadducted T3 (average *m/z* 812.3, +3), IAA-T3 (average *m/z* 831.3, +3), and 1,4-benzoquinone-T3 (average *m/z* 847.7, +3) showed similar ion fragmentation patterns. In each case, singly charged *b* ions dominated the lower *m/z* range of the MS/MS spectra, whereas a series of doubly charged *y* ions were prominent in the higher *m/z* range. Note that the y_{14}^{2+}, y_{15}^{2+}, y_{16}^{2+}, y_{17}^{2+}, and y_{18}^{2+} fragments all contain chemically modified Cys^{34}, and thus have *m/z* values that are characteristic of each adduct. Fragmentation of T3 adducts of 1,4-naphthoquinone, 1,2-phenanthrone, the Cys^{34} sulfonic acid of T3, and estrogen quinones yielded similar MS/MS spectra (supplemental Figs. S1–S4). Based on these results, the b_4^{+}, y_{15}^{2+}, y_{16}^{2+}, and y_{17}^{2+} fragments were chosen to detect T3 adducts in SRM experiments.

Selection of SRM Collision Energies—We used IAA-T3, the sulfonic acid of T3, 1,4-naphthoquinone-T3, and 1,2-phenanthrone-T3 to investigate the relationships between collision energy and SRM signal intensity for each of the four chosen T3 product ions. SRM data were acquired at collision energies ranging from 15 to 41 eV for b_4^{+} and from 15 to 29 eV for the y^{2+} ions. As shown in Fig. 3, the collision energy giving the largest signal for a given product ion did not differ substantially when Cys^{34} was modified by these different electrophiles; the largest deviation of the collision energy at maximum signal was 1–2 eV (lower) for the sulfonic acid of T3 compared with the other adducts. For b_4^{+}, y_{15}^{2+}, y_{16}^{2+}, and y_{17}^{2+} the optimal collision energies were 24, 20, 21, and 21 eV respectively. These collision energies were applied to all SRM experiments.

FS-SRM Transition List and Bin Overflow—A transition list containing 77 theoretical T3 adducts was built with parent ion *m*/z values from 815.0 to 929.0 at increments of 1.5 *m/z* (Supplemental Table S1). Each triply charged parent ion represented an added-mass bin of ±2.3 Da between 9.1 Da and 351.1 Da. Highly abundant parent ions can "overflow" their expected added-mass bins in FS-SRM, thereby contaminating adjacent bins as false positive hits. To investigate this phenomenon, we performed FS-SRM experiments with 1,4-benzoquinone-T3 solutions at concentrations between 1 and 500 nM. The average added mass of benzoquinone-T3 was 107.1 Da for the oxidized (quinone) form and 109.1 Da for the reduced (diol) form, both of which were represented by the same theoretical added mass of 108.1 ± 2.3 Da in FS-SRM. As shown in Fig. 4, hits in the expected 108.1-Da bin were observed over the full range of adduct concentrations. But interestingly, at the two highest concentrations (250 nM and 500 nM), hits were also observed in adjacent bins corresponding to added masses of 103.6 Da and 112.6 Da. This bin-overflow phenomenon should be considered when interpreting FS-SRM results. The results summarized in Fig. 4 suggest that the FS-SRM method has a dynamic range of at least 500-fold (Supplemental Fig. S5).

Detection Rules for Cys^{34} T3 Adducts—Recognizing that false positives can be reduced in SRM methods by matching fragment ion intensities to a predetermined pattern (19), we sought a set of screening rules to guide detection of Cys^{34} T3 modifications. The rules are based upon the geometric means from 200 repetitive measurements of b_4^{+}, y_{15}^{2+}, y_{16}^{2+}, and y_{17}^{2+} fragments for each parent ion in the SRM transition list, measured in both experimental and control (BSA) samples. As shown in Fig. 5, for an experimental parent ion to be considered as a possible Cys^{34} T3 adduct, the lower 95% confidence limits of geometric means for all four of its fragment ions must be greater than the upper 95% confidence limits for the corresponding geometric means of fragment ions in the control (BSA) sample. The remaining detection rules, which were developed with paired samples of synthetic 1,4-benzoquinone-T3 and a control (BSA) are summarized briefly as follows. Because patterns of fragment ions differ between relatively abundant signal intensities and those that approach the detection limit, we first compute the ratio of y_{16}^{2+} intensities between the experimental and control (BSA) samples. If this ratio is greater than or equal to 15, the decision scheme follows the path for high-abundance product ions, shown at left in Fig. 5. In such cases, the unknown is designated as a Cys^{34} T3 adduct if 1) the intensity of the y_{16}^{2+} transition is greater than those of y_{15}^{2+} and y_{17}^{2+}, and 2) the ratio of y_{15}^{2+}/y_{16}^{2+} intensities lies between 0.25 and 0.85. On the other hand, if the ratio of y_{16}^{2+} intensities for experimental and control samples is less than 15, the decision scheme follows the path for low-abundance product ions, shown at right in Fig. 5. Here, the fragment ions y_{15}^{2+}, y_{16}^{2+}, and y_{17}^{2+} are ranked by their intensities and the ratio of the maximum to minimum intensities must be less than 10 for the parent ion to be designated as a Cys^{34} T3 adduct. (Examples of decision rules for the high-abundance and low-abundance pathways are given in supplementary Fig. S6).

We tested the FS-SRM decision rules (Fig. 5) with the following mixture of synthetic Cys^{34} T3 adducts: sulfonic acid of T3 (50 nM), 1,4-benzoquinone-T3 (70 nM), 1,2-phenanthrone-T3 (85 nM), estrogen quinone-T3 (12.5 nM), the diol of estrogen quinone-T3 (50 nM), and an impurity representing estrogen quinone + 16 Da (0.25 nM). Fig. 6 summarizes results in a map of adduct concentration, based upon the

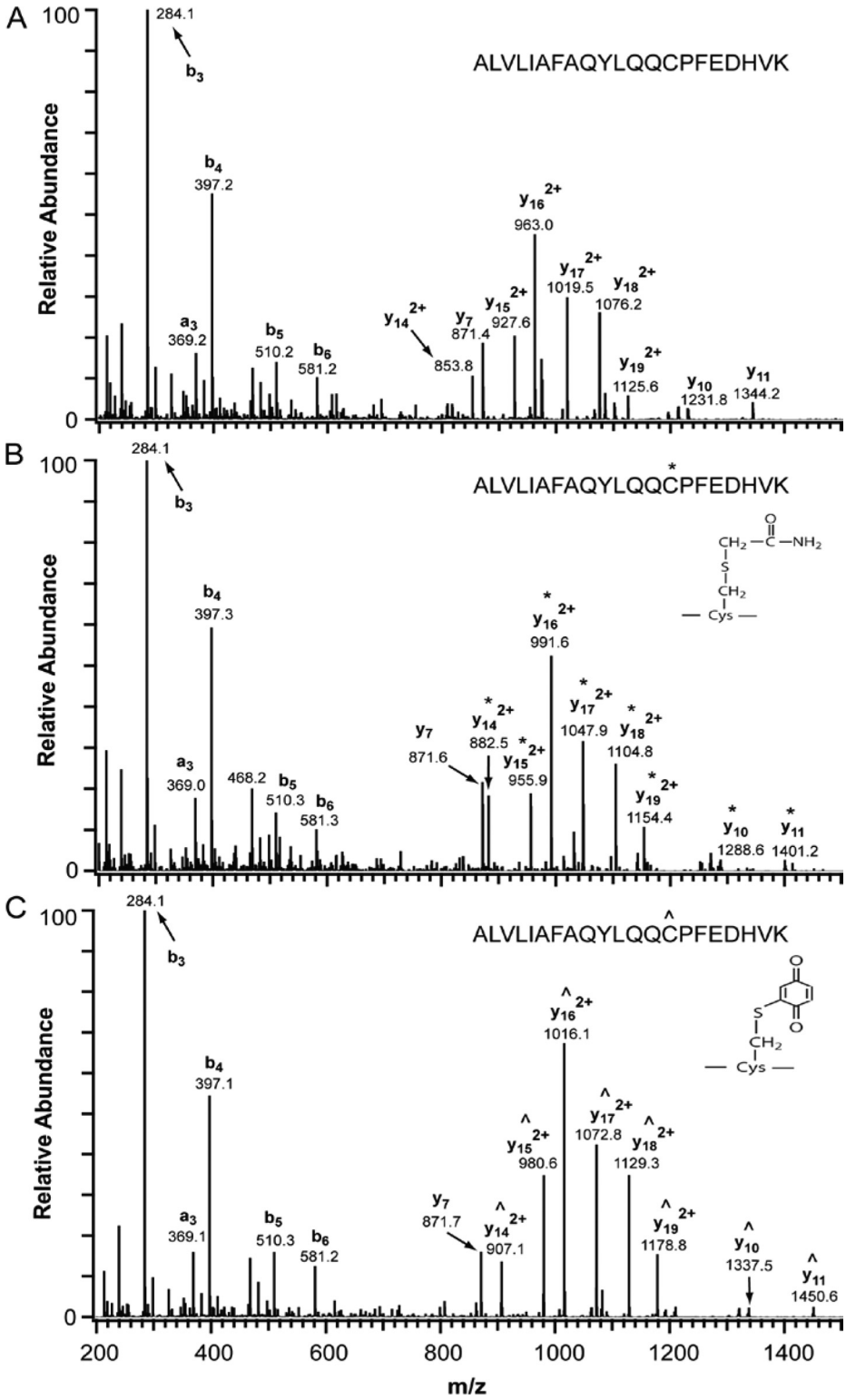

FIG. 2. **MS/MS spectra of T3 (*A*), IAA-T3 (*B*) and 1,4-benzoquinone-T3 (*C*) from TQ-MS.** Sites of adduction by IAA and 1,4-benzoquinone are marked on the T3 peptide with * and ^, respectively. Note the similarity in peak patterns of the doubly charged *y* series ions for the three peptides.

IAA-iT3 internal standard, *versus* added masses from the FS-SRM list. All Cys[34] T3 adducts were successfully detected by FS-SRM and no false positives were observed.

HPLC Purification of HSA Digests—Chromatographic elution times of modified T3 peptides were determined using synthetic T3 adducts. Fig. 7*A* shows the elution profiles of unadducted T3, IAA-T3 and 1,2-phenanthrone-T3. The twin peaks associated with 1,2-phenanthrone-T3 were from reduced (diol) and oxidized (quinone) forms of 1,2-phenanthrone-T3, respectively. Elution times were similar for all

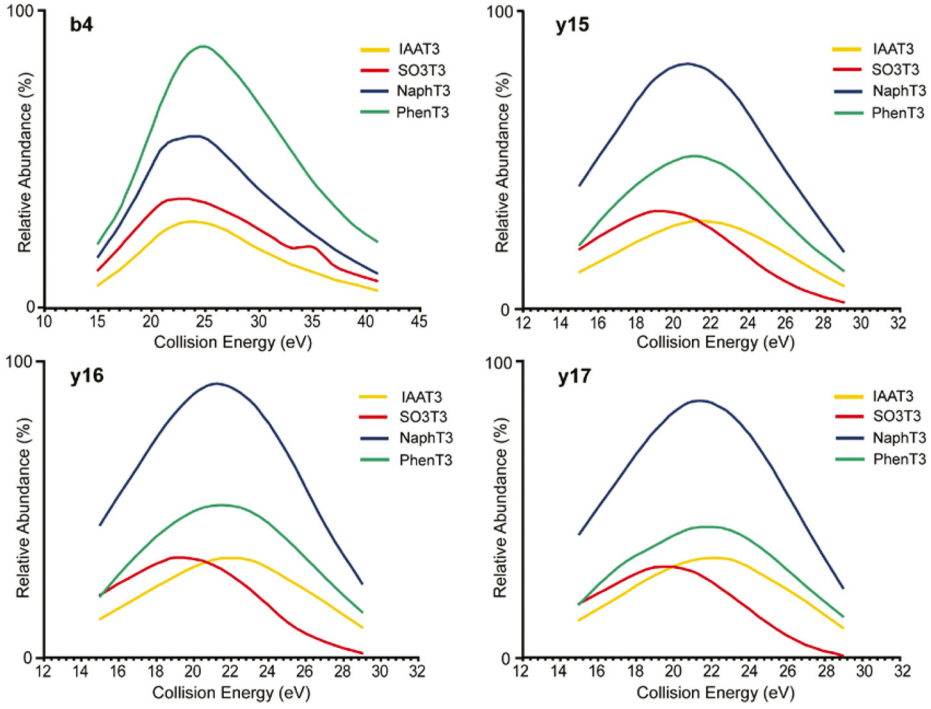

FIG. 3. **Adducted product ion intensities of T3 adducts *versus* the SRM collision energy.** Several adducted T3 peptides were introduced into the MS through static infusion. For each product ion (b_4^{+}, y_{15}^{2+}, y_{16}^{2+} and y_{17}^{2+}), an optimal collision energy is observed, regardless of the particular Cys[34] T3 modification. Legend: IAAT3, iodoacetamide-T3; SO3T3, Cys[34] sulfonic acid of T3; NaphT3, 1,4-naphthoquinone-T3; PhenT3, 1,2-phenanthrone-T3.

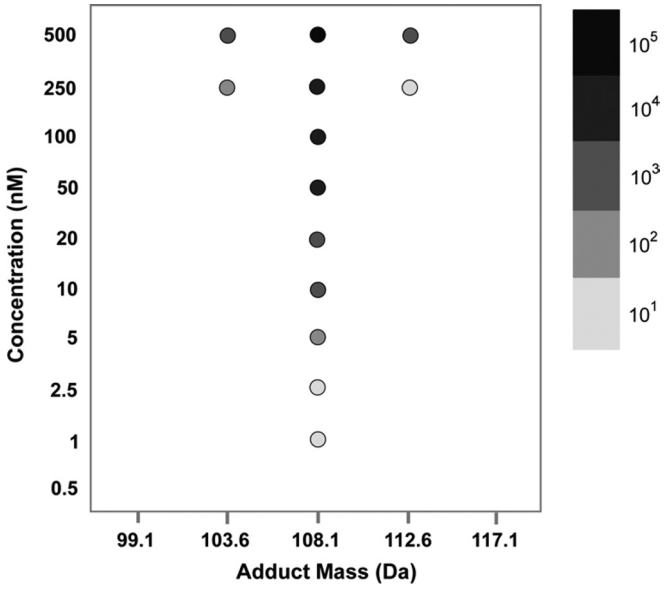

FIG. 4. **Summary of added-mass hits from FS-SRM applied to standards of benzoquinone-T3 at different concentrations.** Only parent ions with added masses close to the theoretical benzoquinone adduct mass (107.1 Da and 109.1 Da for the oxidized and reduced forms, respectively) are shown. Although hits were observed at all adduct concentrations in the expected added-mass bin centered at 108.1 Da, overflow into adjacent bins occurred at the two highest concentrations. The absolute signal intensity of fragment ion y_{16}^{2+} is defined by the gray-scale gradient at right.

tested T3 adducts but increased slightly with the size of the adducting species between 20.0 (IAA-T3) and 21.7 min (estrogen quinones). The elution gradient was applied to the tryptic digests from the 8 archived protein specimens, including duplicate specimens for MWN and MWS, and single specimens for FBN, FBS, MBN and MBS. The hydrophobic T3 peptides were well resolved from most other peptides and impurities (Fig. 7*B*). A slightly expanded time window, from 19.6 to 22.0 min was used for fraction collection to ensure that all Cys[34] T3 adducts were collected.

FS-SRM of T3 Adducts from Human Samples—Following HPLC purification, modified T3 peptide fractions from the human protein samples were analyzed by TQ-MS using FS-SRM to monitor 77 parent ions spanning added masses from 9.1 to 351.1 Da. Results of the FS-SRM experiment are summarized as putative adduct profiles in Fig. 8*A*, after excluding the sodiated and carboxyamidomethylated T3 artifacts at 22.6 and 58.6 Da, respectively. The median number of hits detected from the six specimens of pooled HSA was 69. The FBS and MBS samples contained the most hits (n = 71) whereas that of FBN had the fewest (n = 55). Smokers had somewhat more hits (median = 71) than nonsmokers (median = 63). Median concentrations of hits ranged from 0.28 pmol/mg HSA for FBN (n = 55) to 0.70 pmol/mg HSA for MWS (n = 68) with an overall median concentration of 0.61 pmol/mg HSA (n = 398). Mean concentrations of hits ranged from 10.6 pmol/mg HSA for FBS (n = 71) to 21.4 pmol/mg HSA for MWS (n = 68) with an overall average concentration of 14.4 pmol/mg HSA (n = 398). As shown in Table I, pairs of hits were highly correlated across the 6 HSA specimens, with Spearman coefficients ranging between 0.876 and 0.952.

Our investigation of bin-overflow indicated that adjacent added-mass bins might show false positive hits at concentrations starting between 100 and 250 nM (Fig. 4), which would be equivalent to adduct concentrations between 180 and 448

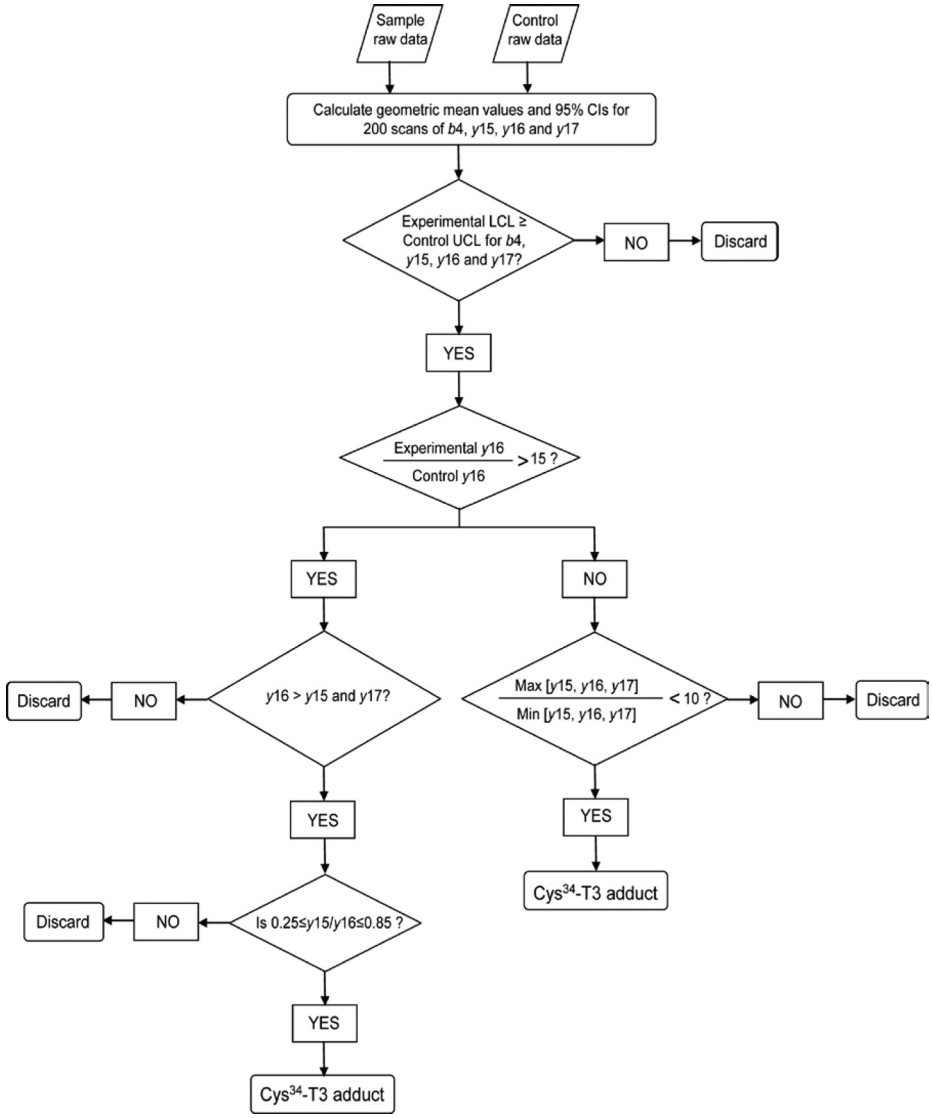

FIG. 5. **Schematic diagram of the decision rules for determining whether a detected product ion should be designated as a putative Cys^{34} T3 adduct.** (See Supplementary Information for illustrated examples).

pmol/mg HSA in our samples (assuming 0.67 mg of HSA as starting material and a final volume of 1.2 ml). As shown in Fig. 8*A*, concentrations of hits exceeded 180 pmol/mg HSA in some samples at added masses of 27.1 Da, 31.6 Da and 81.1 Da. Although this does not necessarily mean that putative T3 adducts detected in mass bins adjacent to these abundant hits are false positives, the estimated concentrations could be less accurate.

Fig. 8*B* shows profiles of cumulative adduct concentrations *versus* the putative adduct mass for the six archived human samples (the cumulative adduct concentration is expressed in the figure as mg adducts/mg HSA, assuming 1 pmol equals 66×10^{-6} mg of each HSA adduct, based upon an assumed mass of 66 kDa for HSA adducts). The more abundant hits, representing about 90% of the cumulative concentrations of all putative adducts, were located in the added-mass range below 100 Da. Two prominent putative adducts were detected in all human samples at added masses of 31.6 Da and 81.1 Da. The sum of all putative adduct concentrations in each sample represented between 0.042 and 0.096 mg/mg HSA, equivalent to between 4.2% and 9.6% of the starting quantities of HSA (Fig. 8*B*). These putative adduct percentages decreased in the order of white males > black males > black females, with smokers having higher percentages than nonsmokers in each category.

Although the adduct profiles were highly correlated between pairs of the six human samples (Fig. 8 and Table I), no statistical conclusions can be drawn regarding differences in a given hit across subject categories because only one sample of pooled HSA was used in each case. Nonetheless, there were suggestive associations between certain hits and sample traits. For example, the hit at 27.1 Da was only found in the three smoker samples whereas that at 72.1 Da was found in three of the four specimens from black subjects (MBN, MBS, and FBN) but not in the white males (MWN and MWS). Also, smokers had higher cumulative concentrations of putative

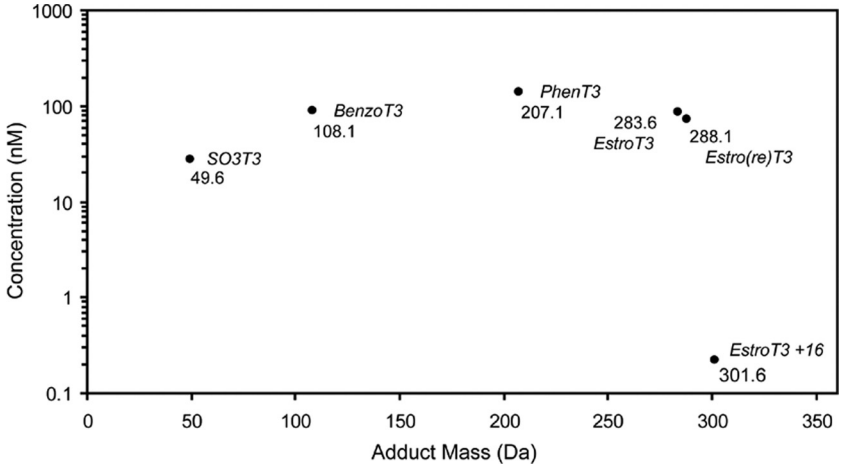

FIG. 6. **Adduct map from fixed-step SRM of a mixture of 6 synthetic Cys^{34} T3 adducts.** The map shows all detected adducts and concentrations estimated from the IAA-iT3 internal standard. Each adduct mass represents the added-mass value from the FS-SRM list with a bin width of ±2.3 Da. Legend: SO3T3, sufonic acid of T3 (adduct mass: 49.0 Da); BenzoT3, 1,4-benzoquinone-T3 (adduct mass: 107.1 Da for the oxidized form and 109.1 for the reduced form); PhenT3, 1,2-phenanthrone-T3 (adduct mass: 207.2 for the quinone form and 209.2 for the diol form); EstroT3, estrogen quinone-T3 (adduct mass: 285.4 Da); Estro(re)T3, estrogen quinone (reduced form)-T3 (adduct mass: 287.4); EstroT3 + 16, an impurity representing the estrogen quinone-T3 adduct +16 Da (adduct mass: 301.4 Da).

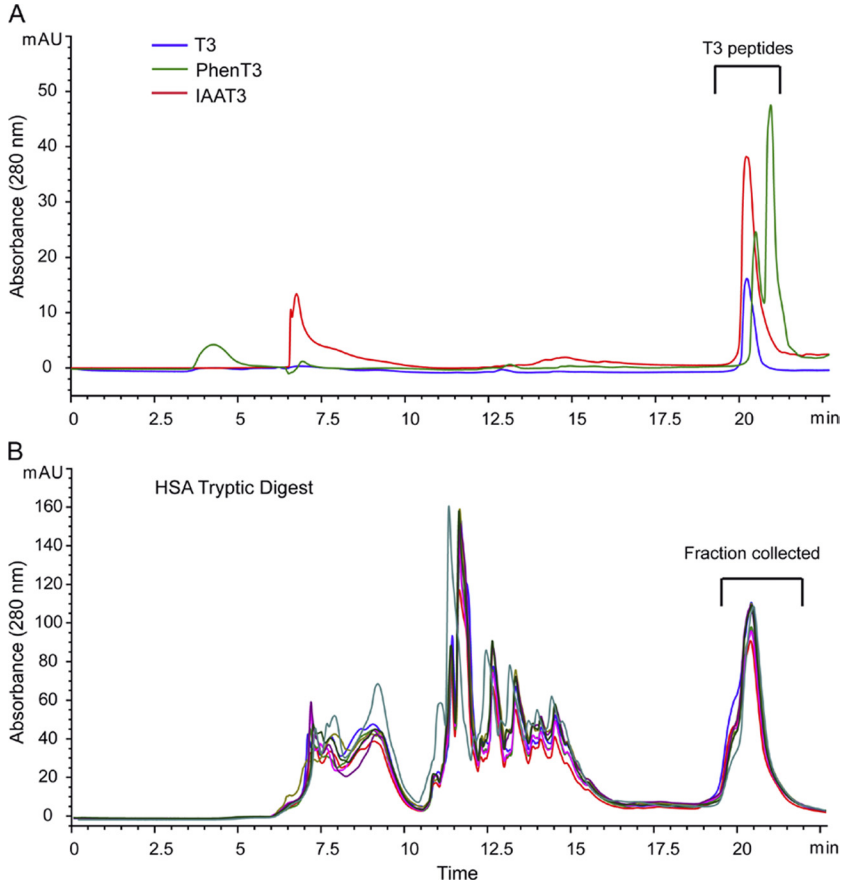

FIG. 7. **Purification of T3 peptides via offline HPLC.** *A*, Overlay of HPLC chromatograms of unadducted T3 (*blue*), IAA-T3 (*red*), and 1,2-phenanthrone-T3 (*green*). *B*, Overlay of chromatograms of eight samples of adduct-enriched tryptic digests of HSA. The T3-adduct fraction was collected from 19.6 to 22.0 min.

adducts than nonsmokers in each subject category (average increase = 26%, range: 17–34%, n = 3 pairs) (Fig. 8*B*).

The precision of FS-SRM quantification was estimated as the average coefficient of variation from all hits in duplicate HSA specimens, which was 26.9% for MWN (n = 63) and 23.1% for MWS (n = 68). Because this coefficient of variation is significantly higher than that of 2.1% observed from replicate analyses of 1,4-BQ-T3 standards, the precision of the method appears to be governed primarily by steps involving adduct enrichment, digestion, and purification, rather than MS.

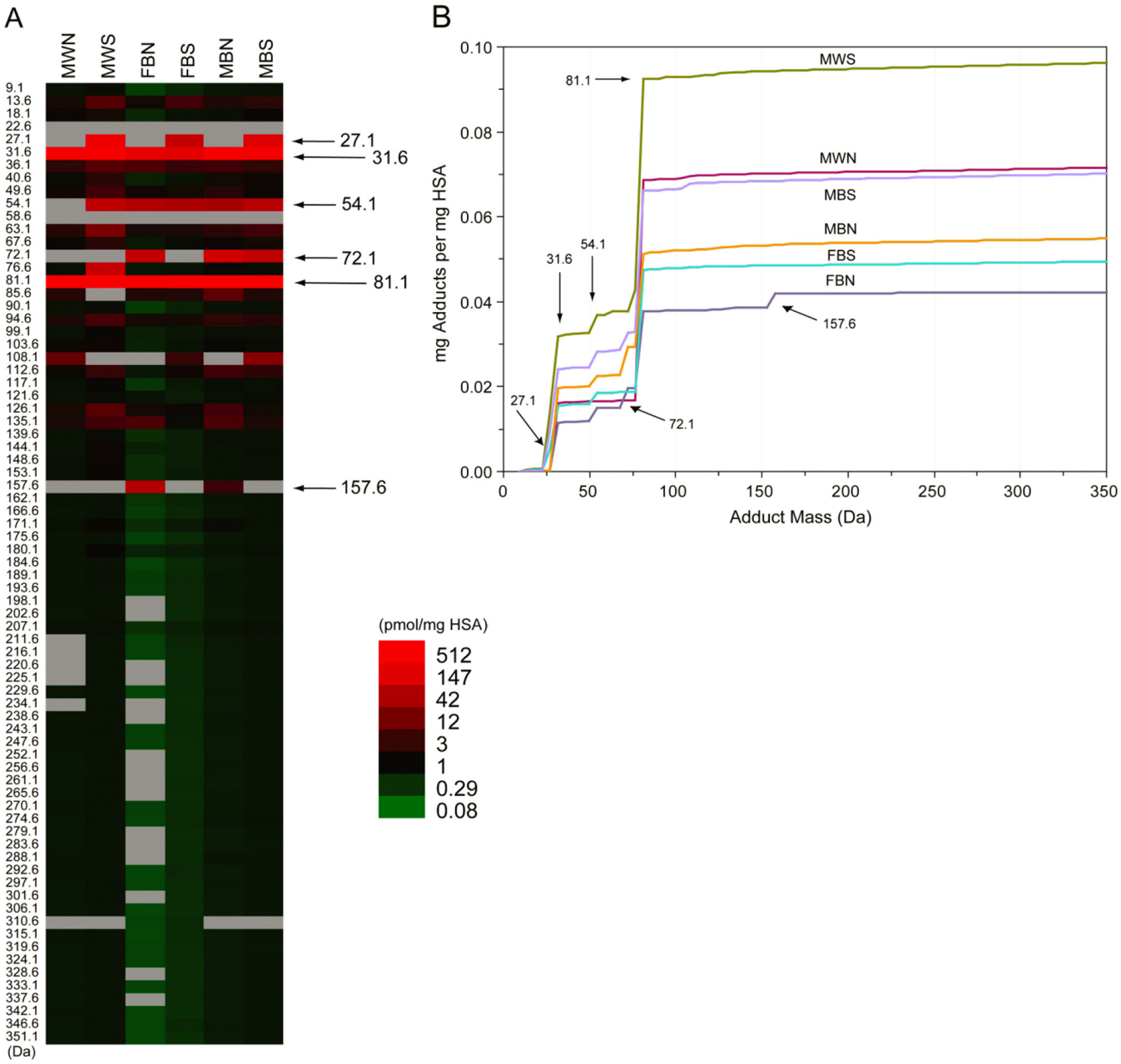

FIG. 8. **Added-mass hits from archived HSA of subjects stratified by race, gender, and smoking status.** Each HSA sample was pooled from five subjects. *A*, Added-mass hits in each HSA sample are shown with estimated concentrations expressed as pmol/mg of HSA (represented by colors). (Concentrations of MWN and MWS are estimated average values from duplicate samples). *B*, Cumulative concentrations of putative HSA adducts expressed as mg Adducts per mg HSA (assuming a uniform HSA-adduct mass of 66 kDa) *versus* the nominal added mass. Added masses that produce relatively large increases in the cumulative concentrations are marked with their corresponding added masses in both (*A*) and (*B*). Legend: M, male; F, female; W, white; B, black; S, smoker; N, nonsmoker.

DISCUSSION

Our interest in profiling HSA-Cys[34] adducts differs from conventional proteomic investigations of post-translational modifications that use MS coupled with modification-specific enrichment techniques. Proteome-wide studies of serine, threonine, and tyrosine phosphorylation (23), lysine acetylation (24), arginine methylation (25), tyrosine nitration (26), and multiple protein targets of known exogenous and endogenous electrophiles (27) have been reported in complex sample matrices. Despite their utility in understanding specific protein modifications, these approaches are not optimal for adduct profiling where the goal is to detect all possible modifications on a given nucleophilic locus of a single protein.

Although TQ-MS SRM methods have detected hundreds of targeted peptides, even at sub-nM concentrations in complex matrices (28, 29), the ability to use SRM to detect untargeted

TABLE I
Correlation of added-mass hits in pooled samples of HSA stratified by race, gender, and smoking status

Spearman coefficients shown with numbers of data pairs in parentheses. Legend: M, male; F, female; W, white; B, black; S, smoker; N, nonsmoker.

	MWS	FBN	FBS	MBN	MBS
MWN	0.901 (61)	0.945 (49)	0.914 (63)	0.902 (62)	0.922 (63)
MWS		0.949 (51)	0.872 (68)	0.887 (67)	0.891 (68)
FBN			0.918 (53)	0.949 (54)	0.952 (53)
FBS				0.892 (68)	0.886 (70)
MBN					0.889 (69)

peptides, has not previously been reported. Indeed, the only applications of FS-SRM of which we are aware are those involving urinary mercapturic acids (11, 12) and DNA nucleosides in autopsy tissues (8, 13), neither of which is directly applicable to profiling unknown modifications of a given protein.

The studies of Wagner *et al.* (11, 12) and Kanaly *et al.* (8, 13) pointed to technical problems with HPLC-TQ-MS-SRM methodology for profiling adducts in human samples. In particular, the ability to reliably scan hundreds (or thousands) of transitions in FS-SRM demands that adduct populations remain constant in the electrospray for sufficient time to achieve statistical stability. Yet, with on-line HPLC, electrospray residence times are just a few seconds—well short of what is needed for precise quantification. In fact, Kanaly *et al.* (8) combined scans from 12 sequential HPLC-TQ-SRM runs to cover a list of 374 transitions, and Wagner *et al.* (12) mentioned data acquisition and processing problems caused by run-to-run differences in HPLC retention times. To overcome these difficulties, we decoupled the HPLC from the MS, and directly infused the chromatographic fraction containing T3 adducts into the MS through a nano-ESI source. This permitted sufficient signal averaging over 21 min to attain the desired 200 repeat scans for each of 312 total transitions.

Another technical issue that was not mentioned in previous applications of FS-SRM relates to the size of each added-mass bin in a list of theoretical transitions. Both Wagner *et al.* (11, 12) and Kanaly *et al.* (8, 13) used transition lists with added-mass increments of one Da. Although the authors recognized that multiple adducts with similar masses could be detected in the same 1-Da bin, they did not mention that the *de facto* mass increment of each bin also depends, in part, upon the resolution of the first quadrupole (Q1) and the abundance of a given adduct in the sample. As the resolution of Q1 decreases and adduct abundance increases, the phenomenon of bin overflow becomes more common and false-positive hits can arise in adjacent mass bins. Thus, there are tradeoffs involving sensitivity, resolution, and abundance that must be considered in designing FS-SRM experiments. In our study of modified HSA-Cys^{34} peptides in ~0.5 mg quantities of enriched HSA, we found that the combination of a 0.7 FWHM Q1 resolution and a bin increment of 1.5 *m/z* minimized effects of bin overflow. Yet, to cover the desired range of adduct masses up to 351 Da, this combination permitted us to investigate only 77 total bins. Although 77 bins are sufficient to prove the concept of protein-adduct profiling, larger bin numbers are desirable to compare putative adduct profiles across populations. This is an area of current research.

We devised screening rules (Fig. 5) to minimize false positive errors in detection of putative T3 adducts. These rules were applied to all monitored transitions (b_4^+, y_{15}^{2+}, y_{16}^{2+}, and y_{17}^{2+}) for each of 77 theoretical parent ions in a FS-SRM experiment. In order to be designated as a putative T3 adduct, all four transitions for a particular parent ion in an experimental sample must first provide statistical evidence that they exceed the corresponding transitions in a paired control (BSA) sample. Then, each set of transitions must also match a set of patterns and intensities that was developed through experimentation with synthetic T3 adducts. Collectively, these decision rules set a high bar for assigning a particular parent ion as a putative adduct. Although SRM results are likely to vary somewhat across TQ-MS platforms, synthetic T3 adducts can be used to develop similar decision rules.

We successfully used FS-SRM to detect six synthetic T3 adducts (with no false positives) at true concentrations between 0.25 and 85 nM (Fig. 4). The observed concentrations of these adducts (Fig. 8) were based upon a single internal standard (IAA-iT3) representing a particular modification (carboxyamidomethylation) of HSA-Cys^{34}. Thus, we implicitly assume that all T3 adducts of equal abundance would produce the same abundance of y_{16}^{2+} signal (the transition used for quantification), regardless of the chemical modification at HSA-Cys^{34}. From our experiments with the six synthetic T3 adducts, the median ratio of observed to true adduct concentrations was 1.36 (range: 0.56 to 6.8). Although this suggests that a typical T3 adduct should have an observed concentration close to the true concentration (*i.e.* within a factor of 1.36), larger biases can occur because of discriminating effects of certain modifications on the ionization and/or charge distribution of product ions, because of differences between nominal and actual added masses, and because of the resolution of Q1. These sources of bias are being further explored.

We detected an average of 66 putative HSA-Cys^{34} adducts in our FS-SRM experiment with six archived specimens of HSA from different categories of subjects based upon race, gender, and smoking status. Concentrations of 398 total hits ranged from 0.2 to 785 pmol/mg HSA, with overall median and mean concentrations of 0.61 and 14.6 pmol/mg HSA, respectively. These putative adduct concentrations are reasonable when compared with results from the few studies that measured targeted HSA-Cys^{34} adducts in human control populations, as summarized by Rubino *et al.* (7) (range of mean adduct concentrations: <0.01–313 pmol/mg HSA for nine targeted adducts). Because the archived blood samples used in our study had been processed in an earlier investigation and stored for 13 years at −80 °C prior to the current

study, we cannot rule out the possibility that some hits resulted from modifications introduced during processing and storage. Nonetheless, our results prove the concept that adducts of HSA-Cys^{34} can be systematically characterized by FS-SRM.

The added-mass range of the hits in our human samples extended from 9.1 to 351.1 Da, with more abundant hits concentrated below 100 Da (Fig. 8*B*). Physiological processes such as the regulation of vascular homeostasis, oxidative stress, and lipid peroxidation generate a wide range of small electrophiles that react with HSA-Cys^{34}, including nitric oxide, small aldehydes, and oxygen radicals (18, 30, 31). Because the thiol of HSA-Cys^{34} resides inside a 10 Å crevice in the HSA molecule (32, 33), the preponderance of small added masses in our sample may also reflect steric restriction of bulky molecules from the reaction site. We recognize that the smallest added mass detected (9.1 Da), is unlikely to represent a simple addition product of HSA-Cys^{34}. Rather, this 9.1-Da moiety could represent either a false positive hit (unlikely because it was detected in all six human samples) or more complex chemistry.

Because cigarette smoke is known to contain about a hundred likely human carcinogens (34), it is, perhaps, surprising that the smoking subjects in our samples had only marginally more putative adduct hits (median = 71) than nonsmokers (median = 63). However, aside from products of nicotine, the carcinogenic constituents of cigarette smoke are also found in effluents from other combustion sources, including vehicular exhausts, and in common foods, such as grilled meats. Also, nonsmokers can be exposed to the same carcinogens from inhalation of environmental tobacco smoke. Nonetheless, smokers tend to be exposed to higher levels of these carcinogens than nonsmokers. Thus, it is interesting that smokers in each of our subject categories had between 17 and 34% higher cumulative concentrations of putative adducts than nonsmokers (Fig. 8*B*). Differences of this magnitude are consistent with results from the few studies that reported concentrations of targeted HSA-Cys^{34} adducts in smokers and nonsmokers, namely, those of benzene oxide (0.113 pmol/mg HSA in nonsmokers *versus* 0.094 pmol/mg HSA in smokers) (35), 1,4-benzoquinone (0.687 pmol/mg HSA in nonsmokers *versus* 0.760 pmol/mg HSA in smokers) (36), styrene-7,8-oxide (2.54 pmol/mg HSA in nonsmokers *versus* 3.49 pmol/mg HSA in smokers) (37), 1,4-naphthoquinone (0.045 pmol/mg HSA in nonsmokers *versus* 0.061 pmol/mg HSA in smokers) (38), 1,2-naphthoquinone (0.056 pmol/mg HSA in nonsmokers *versus* 0.062 pmol/mg HSA in smokers (38), and the *N*-nitroso metabolite of 2-amino-1-methyl-6-phenylimidazo[4,5-b]pyridine (PhIP) (0.005 pmol/mg HSA in nonsmokers *versus* 0.005 pmol/mg HSA in smokers) (39).

In summary, we developed a MS method, termed FS-SRM, that enables profiling of unknown HSA-Cys^{34} adducts with masses up to 351 Da. Using a set of known HSA-Cys^{34} adducts, we established structured rules to guide detection of putative adducts while minimizing false positive detection. To validate the method, we recorded putative adduct profiles from six samples of archived HSA, pooled from subjects stratified by race, gender and smoking status (Fig. 8*A*). Putative HSA-Cys^{34} adducts covered a wide range of concentrations, were most abundant in the mass range below 100 Da, and were more abundant in smokers than in nonsmokers. With minor modifications, this method can be used to compare adduct profiles across populations of interest and is sufficiently general to be applied to other nucleophilic sites and proteins.

Acknowledgments—We thank Anthony Iavarone and Ulla Norklit Andersen, of the University of California, Berkeley QB3 Institute, for technical assistance with mass spectrometry and Suramya Waidyanatha for discussions regarding adduct analysis. We are grateful to Jimmy Eng at the Institute for Systems Biology for assistance with customizing data-analysis software.

* This work was supported by grant U54ES016115 from the U.S. National Institute for Environmental Health Sciences (NIEHS) through the trans-National Institutes of Health (NIH) Genes, Environment, and Health Initiative and by NIEHS training grant T32ES07018. The content is solely the responsibility of the authors and does not necessarily represent the official view of the NIEHS or the NIH.

S This article contains supplemental Table S1 and Figs. S1–S6.

‖ To whom correspondence should be addressed: School of Public Health, University of California, Berkeley, CA 94720, USA. Tel.: 510-642-4355; Fax: 510-642-0427; E-mail: srappaport@berkeley.edu.

REFERENCES

1. Brodie, B. B., Reid, W. D., Cho, A. K., Sipes, G., Krishna, G., and Gillette, J. R. (1971) Possible mechanism of liver necrosis caused by aromatic organic compounds. *Proc. Natl. Acad. Sci. U.S.A.* **68,** 160–164
2. Miller, E. C., and Miller, J. A. (1966) Mechanisms of chemical carcinogenesis: nature of proximate carcinogens and interactions with macromolecules. *Pharmacol. Rev.* **18,** 805–838
3. Dalle-Donne, I., Rossi, R., Colombo, R., Giustarini, D., and Milzani, A. (2006) Biomarkers of oxidative damage in human disease. *Clin. Chem.* **52,** 601–623
4. Liebler, D. C. (2008) Protein damage by reactive electrophiles: targets and consequences. *Chem. Res. Toxicol.* **21,** 117–128
5. Sayre, L. M., Perry, G., and Smith, M. A. (2008) Oxidative stress and neurotoxicity. *Chem. Res. Toxicol.* **21,** 172–188
6. Törnqvist, M., Fred, C., Haglund, J., Helleberg, H., Paulsson, B., and Rydberg, P. (2002) Protein adducts: quantitative and qualitative aspects of their formation, analysis and applications. *J. Chromatogr. B Analyt. Technol. Biomed. Life Sci.* **778,** 279–308
7. Rubino, F. M., Pitton, M., Di Fabio, D., and Colombi, A. (2009) Toward an "omic" physiopathology of reactive chemicals: Thirty years of mass spectrometric study of the protein adducts with endogenous and xenobiotic compounds. *Mass Spectrom Rev.* **25(8),** 725–784
8. Kanaly, R. A., Hanaoka, T., Sugimura, H., Toda, H., Matsui, S., and Matsuda, T. (2006) Development of the adductome approach to detect DNA damage in humans. *Antioxid. Redox. Signal* **8,** 993–1001
9. Merrick, B. A. (2008) The plasma proteome, adductome and idiosyncratic toxicity in toxicoproteomics research. *Brief Funct. Genomic Proteomic* **7,** 35–49
10. Rappaport, S. M., and Smith, M. T. (2010) Environment and disease risks. *Science* **330,** 460–461
11. Wagner, S., Scholz, K., Donegan, M., Burton, L., Wingate, J., and Völkel, W. (2006) Metabonomics and biomarker discovery: LC-MS metabolic profiling and constant neutral loss scanning combined with multivariate data analysis for mercapturic acid analysis. *Anal Chem* **78,** 1296–1305
12. Wagner, S., Scholz, K., Sieber, M., Kellert, M., and Voelkel, W. (2007) Tools in metabonomics: an integrated validation approach for LC-MS meta-

bolic profiling of mercapturic acids in human urine. *Anal. Chem.* **79,** 2918–2926
13. Kanaly, R. A., Matsui, S., Hanaoka, T., and Matsuda, T. (2007) Application of the adductome approach to assess intertissue DNA damage variations in human lung and esophagus. *Mutat. Res.* **625,** 83–93
14. Lindstrom, A. B., Yeowell-O'Connell, K., Waidyanatha, S., McDonald, T. A., Golding, B. T., and Rappaport, S. M. (1998) Formation of hemoglobin and albumin adducts of benzene oxide in mouse, rat, and human blood. *Chem. Res. Toxicol.* **11,** 302–310
15. Yeowell-O'Connell, K., Jin, Z., and Rappaport, S. M. (1996) Determination of albumin and hemoglobin adducts in workers exposed to styrene and styrene oxide. *Cancer Epidemiol. Biomarkers Prev.* **5,** 205–215
16. Yeowell-O'Connell, K., Rothman, N., Waidyanatha, S., Smith, M. T., Hayes, R. B., Li, G., Bechtold, W. E., Dosemeci, M., Zhang, L., Yin, S., and Rappaport, S. M. (2001) Protein Adducts of 1,4-Benzoquinone and Benzene Oxide among Smokers and Nonsmokers Exposed to Benzene in China. *Cancer Epidemiol. Biomarkers Prev.* **10,** 831–838
17. Aldini, G., Gamberoni, L., Orioli, M., Beretta, G., Regazzoni, L., Maffei Facino, R., and Carini, M. (2006) Mass spectrometric characterization of covalent modification of human serum albumin by 4-hydroxy-trans-2-nonenal. *J. Mass Spectrom.* **41,** 1149–1161
18. Aldini, G., Vistoli, G., Regazzoni, L., Gamberoni, L., Facino, R. M., Yamaguchi, S., Uchida, K., and Carini, M. (2008) Albumin is the main nucleophilic target of human plasma: a protective role against pro-atherogenic electrophilic reactive carbonyl species? *Chem. Res. Toxicol.* **21,** 824–835
19. Gupta, M. K., Jung, J. W., Uhm, S. J., Lee, H., Lee, H. T., and Kim, K. P. (2009) Combining selected reaction monitoring with discovery proteomics in limited biological samples. *Proteomics* **9,** 4834–4836
20. Funk, W. E., Li, H., Iavarone, A. T., Williams, E. R., Riby, J., and Rappaport, S. M. (2010) Enrichment of cysteinyl adducts of human serum albumin. *Anal. Biochem.* **400,** 61–68
21. de Hoon, M. J. L., Imoto, S., Nolan, J., and Miyano, S. (2004) Open source clusturing software. *Bioinformatics* **20,** 1453–1454
22. Saldanha, A. J. (2004) Java Treeview–extensible visualization of microarray data. *Bioinformatics* **20,** 3246–3248
23. Olsen, J. V., Blagoev, B., Gnad, F., Macek, B., Kumar, C., Mortensen, P., and Mann, M. (2006) Global, in vivo, and site-specific phosphorylation dynamics in signaling networks. *Cell* **127,** 635–648
24. Zhang, J., Sprung, R., Pei, J., Tan, X., Kim, S., Zhu, H., Liu, C. F., Grishin, N. V., and Zhao, Y. (2009) Lysine acetylation is a highly abundant and evolutionarily conserved modification in Escherichia coli. *Mol. Cell Proteomics* **8,** 215–225
25. Ong, S. E., Mittler, G., and Mann, M. (2004) Identifying and quantifying in vivo methylation sites by heavy methyl SILAC. *Nat. Methods* **1,** 119–126
26. Zhan, X., and Desiderio, D. M. (2006) Nitroproteins from a human pituitary adenoma tissue discovered with a nitrotyrosine affinity column and tandem mass spectrometry. *Anal. Biochem.* **354,** 279–289
27. Liebler, D. C. (2002) Proteomic approaches to characterize protein modifications: new tools to study the effects of environmental exposures. *Environ. Health Perspect.* **110** Suppl **1,** 3–9
28. Anderson, L., and Hunter, C. L. (2006) Quantitative mass spectrometric multiple reaction monitoring assays for major plasma proteins. *Mol. Cell Proteomics* **5,** 573–588
29. Stahl-Zeng, J., Lange, V., Ossola, R., Eckhardt, K., Krek, W., Aebersold, R., and Domon, B. (2007) High sensitivity detection of plasma proteins by multiple reaction monitoring of N-glycosites. *Mol. Cell Proteomics* **6,** 1809–1817
30. Tsikas, D., Sandmann, J., and Frolich, J. C. (2002) Measurement of S-nitrosoalbumin by gas chromatography–mass spectrometry. III. Quantitative determination in human plasma after specific conversion of the S-nitroso group to nitrite by cysteine and Cu(2+) via intermediate formation of S-nitrosocysteine and nitric oxide. *J. Chromatogr. B Analyt. Technol. Biomed. Life Sci*. **772,** 335–346
31. Turell, L., Botti, H., Carballal, S., Radi, R., and Alvarez, B. (2009) Sulfenic acid–a key intermediate in albumin thiol oxidation. *J. Chromatogr. B Analyt. Technol. Biomed. Life Sci.* **877,** 3384–3392
32. He, X. M., and Carter, D. C. (1992) Atomic structure and chemistry of human serum albumin. *Nature* **358,** 209–215
33. Christodoulou, J., Sadler, P. J., and Tucker, A. (1995) 1H NMR of albumin in human blood plasma: drug binding and redox reactions at Cys34. *FEBS Lett.* **376,** 1–5
34. Smith, C. J., Perfetti, T. A., Garg, R., and Hansch, C. (2003) IARC carcinogens reported in cigarette mainstream smoke and their calculated log P values. *Food Chem. Toxicol.* **41,** 807–817
35. Yeowell-O'Connell, K., Rothman, N., Smith, M. T., Hayes, R. B., Li, G., Waidyanatha, S., Dosemeci, M., Zhang, L., Yin, S., Titenko-Holland, N., and Rappaport, S. M. (1998) Hemoglobin and albumin adducts of benzene oxide among workers exposed to high levels of benzene. *Carcinogenesis* **19,** 1565–1571
36. Lin, Y. S., McKelvey, W., Waidyanatha, S., and Rappaport, S. M. (2006) Variability of albumin adducts of 1,4-benzoquinone, a toxic metabolite of benzene, in human volunteers. *Biomarkers* **11,** 14–27
37. Fustinoni, S., Colosio, C., Colombi, A., Lastrucci, L., Yeowell-O'Connell, K., and Rappaport, S. M. (1998) Albumin and hemoglobin adducts as biomarkers of exposure to styrene in fiberglass-reinforced-plastics workers. *Int. Arch. Occup. Environ. Health* **71,** 35–41
38. Waidyanatha, S., Zheng, Y., Serdar, B., and Rappaport, S. M. (2004) Albumin adducts of naphthalene metabolites as biomarkers of exposure to polycyclic aromatic hydrocarbons. *Cancer Epidemiol. Biomarkers Prev.* **13,** 117–124
39. Magagnotti, C., Orsi, F., Bagnati, R., Celli, N., Rotilio, D., Fanelli, R., and Airoldi, L. (2000) Effect of diet on serum albumin and hemoglobin adducts of 2-amino-1-methyl-6-phenylimidazo[4,5-b]pyridine (PhIP) in humans. *Int. J. Cancer* **88,** 1–6